

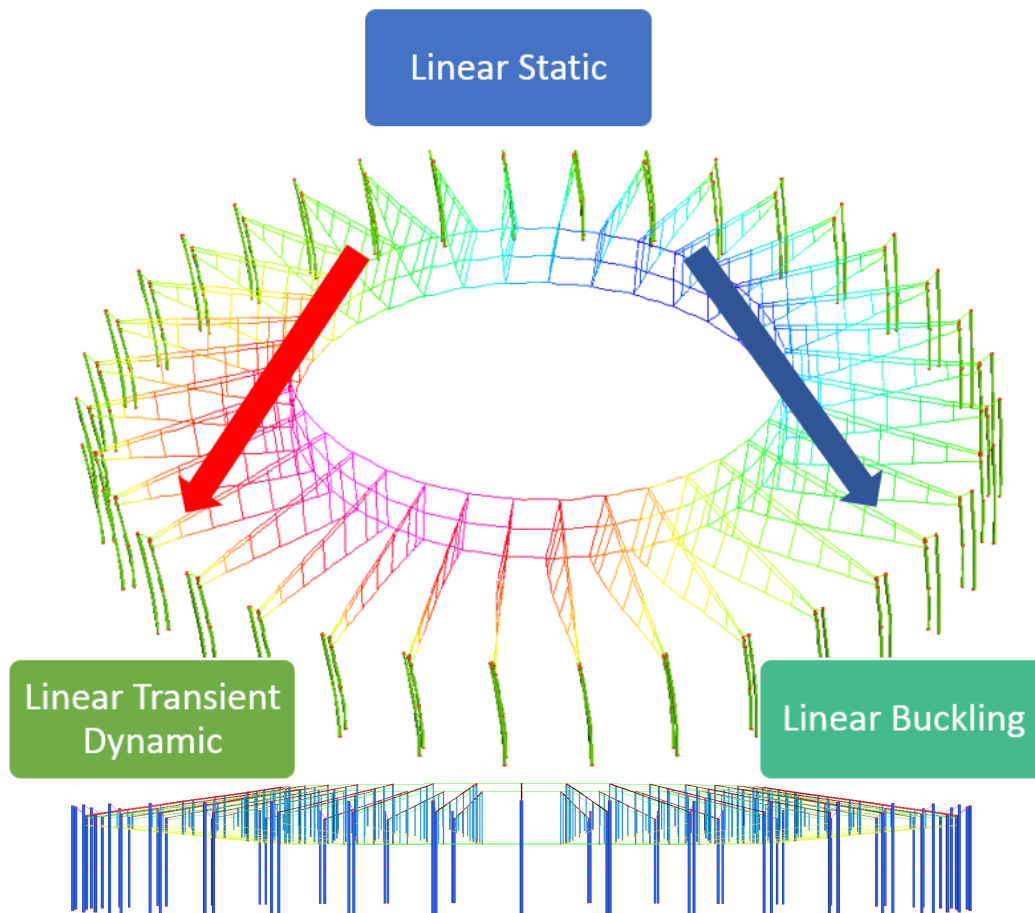
Transient Dynamic Analysis of the Bao'An Stadium

David Knight, Rowan Whitefield, Eric Nhieu, Faham Tahmasebinia, Peter Ansourian, and Fernando Alonso-Marroquin ^{a)}

School of Civil Engineering, the University of Sydney, Sydney NSW 2006

^{a)}Corresponding author: fernando@sydney.edu.au

Abstract. Bao'An Stadium is a unique structure that utilises 54m span cantilevers with tensioned members to support the roof. This report involves a simplified finite element model of Bao'An stadium using Strand7 to analyse the effects of deflections, buckling and earthquake loading. Modelling the cantilevers of the original structure with a double curvature was problematic due to unrealistic deflections and no total mass participation using the Spectral Response Solver. To rectify this, a simplified symmetrical stadium was created and the cable free length attribute was used to induce tension in the inner ring and bottom chord members to create upwards deflection. Further, in place of the Spectral Response Solver, the Transient Linear Dynamic Solver was inputted with an El-Centro earthquake. The stadium's response to a 0.20g earthquake and self-weight indicated the deflections satisfied AS1170.0, the loading in the columns was below the critical buckling load, and all structural members satisfied AS4100.



INTRODUCTION

Bao'An stadium is an iconic structure that has structural columns inspired by local bamboo forests, intended to create a prominent feature in Shenzhen China. The structure has a circular shape with an outer diameter of 236m and an inner diameter of 128m. A lightweight roof structure with a polytetrafluoroethylene membrane is cantilevered 54m to provide shelter for spectators. The stadium is a complex structure due to the inclusion of the inner ring cables that have a pre tension of 3600 kN in the top cable, and 1800 kN in the bottom cable. These cables are supported through a lightweight truss system comprising of thin cables that extend to the external columns which also support a large compression ring. The columns are large circular hollow sections ranging in sizes from 550 mm to 800 mm. The stadium behaves similar to a bicycle wheel, the trusses equivalent to tension spokes of the wheel and the rim representing the outer compression ring (Guo et al., 2011; Tian et al., 2011). The stadium has a gross floor area of 88,500 m² and was constructed over a 2 year period. TABLE 1 shows the main details.

The key structural components supporting the stadium roof are long span cantilevered members. This is achieved through the use of tensioned cables as the bottom chord and a tapered truss geometry that creates upward deflection (Guo et al., 2013). This report investigates how the cantilevers of Bao'An stadium prevent deflections under self-weight and dynamic earthquake loading.

TABLE 1. Building details

Location: Shenzhen China	The year of build: 2009-2011
Architects: GMP Architekten	Overall height: 39.65m
Structural Engineers: Schlaich Bergermann Und Partner	Floor area: 88,500 m ²
Function: Sports stadium primarily constructed for the Universiade	Car spaces: 750
The structure of the plan: A large circular roof structure with a circular rings at the centre supported on a complicated external column geometry ranging from 550 mm to 800 mm	Occupant capacity: 40,050

PRELIMINARY STRUCTURAL MEMBERS

There is a lack of detailed information in the literature on the member sizing and properties. This resulted in the majority being estimated from pictures. The members chosen for the Strand7 model were based on images from Ferguson (2011) and structural journals (Guo et al., 2011; Guo et al., 2013; Tian et al., 2011). TABLE 2 shows the members chosen for the structure. The detailed member selection process is contained in APPENDIX 1. The key criteria for the selection of the members was vertical deflection limits, ideally stiff, light weight members. This is achieved with the selection of circular hollow sections for majority of the structural members.

TABLE 2. Structural elements

Structural Element	Size of elements (mm)	Dead Load (kN/m)
External Columns	800x50 CHS	9.07
Box Girder	200 x 100	1.54
Top Chord	250 x 30 CHS	1.60
Bottom Chord	200 x 5 CHS	0.24
Cables	10 mm Cable	-
Vertical Truss Members	400 x 10 CHS	-
Roof Membrane - polytetrafluoroethylene	1mm	0.20

STRUCTURAL SYSTEM

Bao'An stadium consists of a complex structural system to resist vertical and lateral loads. Vertical loads are resisted as shear flows through the roof truss. These are then transferred to the columns as bending moments through a fixed connection, and then transferred to the foundations. The membrane roof is connected continuously to the top chord to completely suppress all buckling modes. Vertical truss members also act as spring stiffeners to reduce the effective length to the lower chord to prevent large buckling modes. The ring cables are pre tensioned to prevent any compressive stresses causing sagging catenary actions. Lateral loads are resisted by the very stiff columns which are stabilised by the outer compression rings.

Long Span Cantilever

To demonstrate how the cantilevers can resist deflection, a single column-roof section has been analysed. The self-weight of all the roof members are treated as an applied uniformly distributed load on the top chord. The bottom chord is pre-tensioned to prevent compressive stresses while the inner ring is in tension to limit deflections. FIGURE 1(a) shows the overall action of the tensioned cables in the bottom chord and bottom inner ring. The net resultant force is acting inwards because the inner ring is tensioned higher. FIGURE 1(b), shows a free body diagram of a typical column-roof section with the applied tensile force 'T' as the resultant action of cable tension, this tensile force T may be chosen to minimise the deflection of the cantilever. FIGURE 1(c) shows how this effectively creates an applied moment that resists deflection.

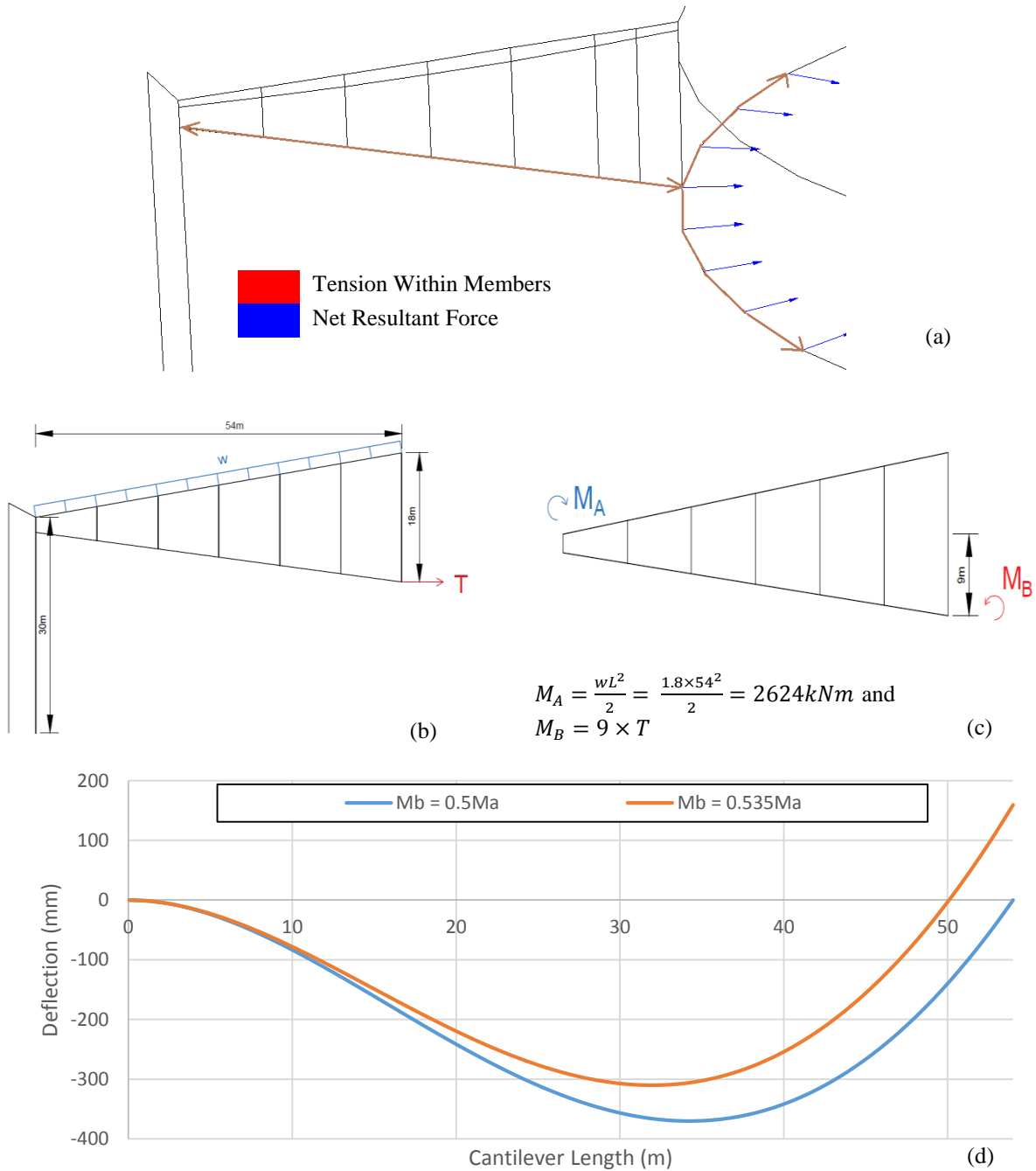


FIGURE 1. (a) Net resultant force of single section (b) Free body diagram of a column-roof section (c) Free body diagram of a truss cantilever (d) Comparison of deflected shape with applied end moment

The truss is treated as a cantilevered beam with constant second moment of area, it can be shown that the moment EQUATION (1) can be integrated twice (2) for deflection:

$$M(x) = \frac{w}{2}(x^2 - 2L) - M_b \quad (1)$$

$$v(x) = \iint -\frac{M}{EI} dx = -\frac{wx^2}{24EI}(x^2 - 4xL + 6L^2) + \frac{M_b x^2}{EI} \quad (2)$$

The cantilevered beam is assumed to have a depth of 9m as shown in FIGURE 1(b). The stiffness was then calculated using the parallel axis theorem. A model was created to visualise the deflected shape and optimised the applied moment M_B to an appropriate value. In FIGURE 1(d) it was found that zero deflection at the free end of the cantilever occurred when the end moment was half the support moment, $M_B = 0.5M_A$. Further, through trial and error the sagging and hogging deflections were minimised, at a value of $M_B = 0.535M_A$. The resulting deflections were -295.6 mm downward and 230.9 mm upward with a theoretical tensile value of 156.00 kN.

$$M_B = 0.535M_A = 0.535 \times 2624 = 1403 \text{ kNm} \quad (3)$$

$$T = \frac{M_B}{9\text{m}} = \frac{1404 \text{ kNm}}{9\text{m}} = 156.00 \text{ kN} \quad (4)$$

DESIGN AIMS

Deflection

The key parameter in the design was to limit the deflections experienced in the 54m cantilever. The process involved modelling a singular column section and optimising the structure with cable elements to effectively reduce the deflections. Once the deflections were satisfied, the stresses were checked and a buckling analysis was done. The structure was then copied every 10° about the vertical axis to complete the model. The guide for acceptable deflections is stated in AS1170.0 as EQUATION 5;

$$\delta = \frac{L}{120} = \frac{54}{120} = 0.45\text{m} \quad (5)$$

Buckling Analysis

Perfect Euler

The column was assumed to be a vertical cantilever with restraints at the top to be free and the bottom to be translation and rotation fixed. The buckling length of the column was assumed to be half in EQUATION 6:

$$P = \frac{\pi^2 EI}{4L^2} = \frac{\pi^2 \times 200000 \times 8.32 \times 10^9}{4 \times (32000)^2} = 4010 \text{ kN} \quad (6)$$

Strand7 – Linear Buckling Analysis

The first mode of buckling was done with no gravity and then gravity applied. The eigenvalue and critical buckling loads were found by strand7 using EQUATION 7.

$$P_{applied} \times \lambda = P_{crit} \quad (7)$$

Earthquake Analysis

For a transient solver with damping, the global matrix equation is listed as EQUATION 8 below where M, C, and K are the mass, damping and stiffness matrices respectively. $Mrg(t)$ represents the external force (base acceleration) acting on the mass where r is an arbitrary vector and g(t) is the earthquake acceleration.

$$M\ddot{U} + C\dot{U} + KU = Mrg(t) \quad (8)$$

Before applying an earthquake, the structure was observed to be oscillating. To reduce oscillations, Rayleigh damping was applied and the earthquake was run at 600 seconds after the initial vibrations were sufficiently damped. It was found that the spectral response solver solutions produced mass participation factors of zero. The assumption of a combination of modal shapes was not applicable hence the need for a Transient Dynamic Solver.

METHODOLOGY

Cylindrical Coordinates & Online Editor for 3D Model

In Strand7, a single 2D column was created according to the nodes and elements in FIGURE 2. To create a 3D model, the online editor tool was used to import the coordinates of the nodes for the columns and inner ring beams from a spreadsheet. The nodes for the columns and ring beams were set every 10° and the appropriate beam elements were selected as per (Guo et al., 2013). Using this process, the column section in FIGURE 2 was copied around a central axis to form the completed 3D model of the stadium as shown in FIGURE 3.

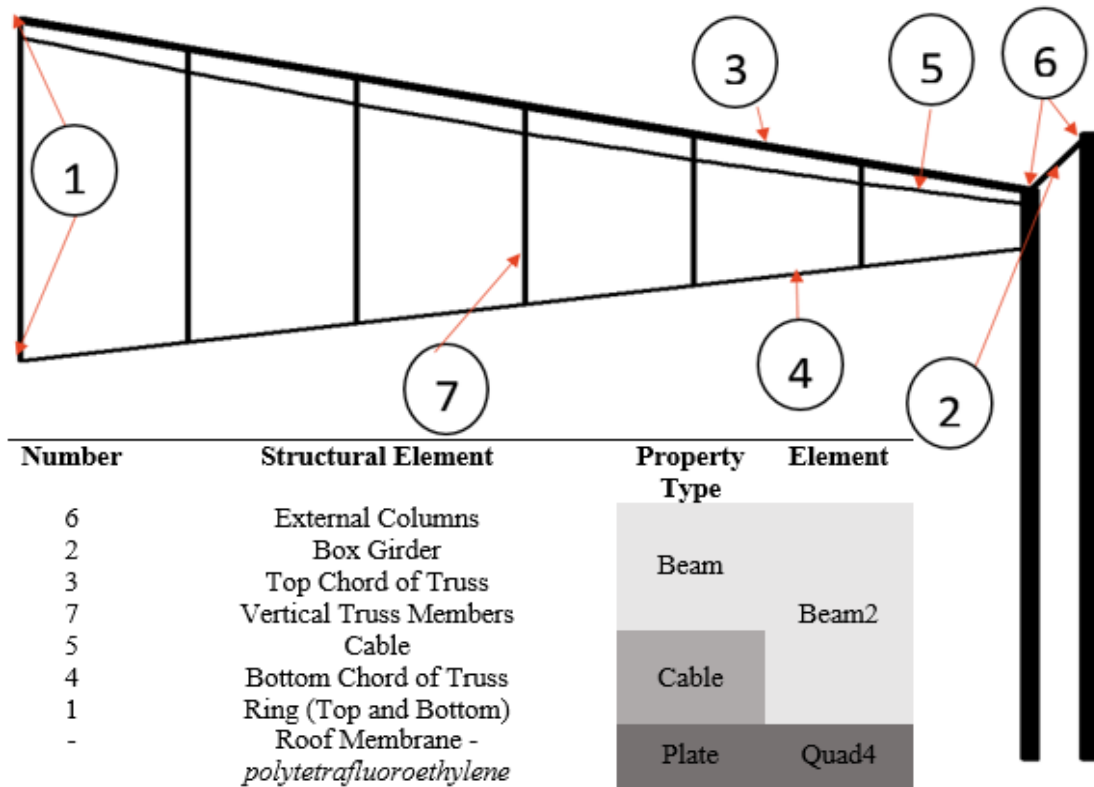


FIGURE 2. Schematic of structural members

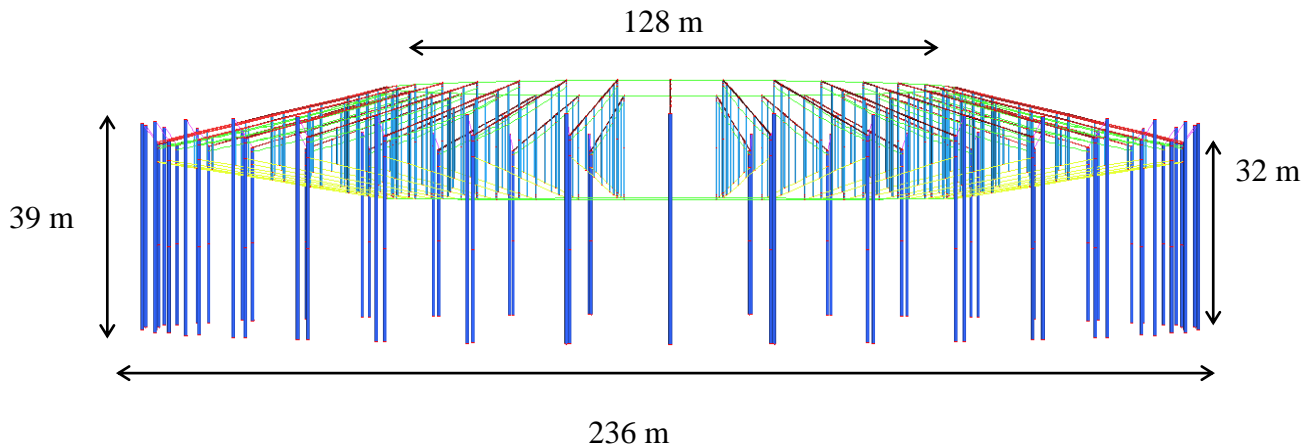


FIGURE 3. Section view

Modelling Limitations

In this model, the roof was lighter than the actual stadium due to purlins that are supporting the Teflon roof not being modelled. It could be expected that the required cable tension would be higher than the value obtained from Strand7.

The double curvature of the roof was ignored to allow for a simple structure resembling a cantilever spanning 54m. The flat roof allowed for each cantilever section to deflect equally. In an initial model, incorporating the curves in the roof resulted in collapse.

The outer ring beams were not included in the model since they proved to be redundant in minimising deflections. The columns are significantly large and the box girder connecting the beams provided sufficient restraint.

Cable Elements

Cable elements required a non-linear analysis due to the deformed geometry of the cable. In the linear static analysis, the load in the cable acted in the vertical direction only. In the nonlinear analysis the load is applied on the deformed shape so it has orthogonal and parallel components to the cable. The effect of having the parallel component is that axial shortening occurs. When running the nonlinear solver, the vertical deflection increased by 2mm and was not significant.

To reduce deflections, the Cable Free Length attribute is a key parameter that can be modified to induce tension in the cable elements. The Cable Free Length of the bottom chord was chosen to be 8m with the original cable length as 8.55m. The Cable Free Length of the bottom inner ring beam was chosen to be 9.5m given the actual length is 11.5m.

The second method for inducing tension in cable members is applying point loads. Radial point loads were applied which effectively mimicked the pre tension within the members as shown in FIGURE 1(a). Through this method, a loading of 565 kN was applied which resulted in a similar deflection of 140mm. The reason this method was not selected as it made the inner cables redundant as no load was being carried.

Linear Transient Dynamic Solver

To model the stadium's response to an earthquake, the El Centro earthquake data was used. The ground acceleration was similar to that expressed in the Chinese standard GB 50011-2011 which specified 0.2g. The acceleration vs time graphs for x, y and z were inputted as the base acceleration in the solver. The earthquake was applied at 600 seconds after the initial vibrations were sufficiently damped.

NUMERICAL ANALYSIS

Linear Buckling

A load case without gravity was computed to compare with the Perfect Euler mode of buckling. The eigenvalue converged on the first iteration as expected and P_{crit} was found to be 4039 kN. To find P_{crit} with gravity an initial load of 1 kN was applied and followed by six iterations. The results are summarised in the TABLE 3. Gravity induces extra compressive stresses so the column buckles earlier than perfect Euler.

TABLE 3. Buckling Analysis

Iteration	Force (kN)	Eigenvalue for Mode 1
1	1.0	27.650
2	27.6	23.384
3	646.6	5.103
4	3299.4	1.173
5	3869.6	1.006
6	3893.8	1.000
Buckling (Perfect Euler) 4010 kN	Buckling (Strand7 Gravity) 3894 kN	Buckling (Strand7 No Gravity) 4039 kN

Linear Static Solver

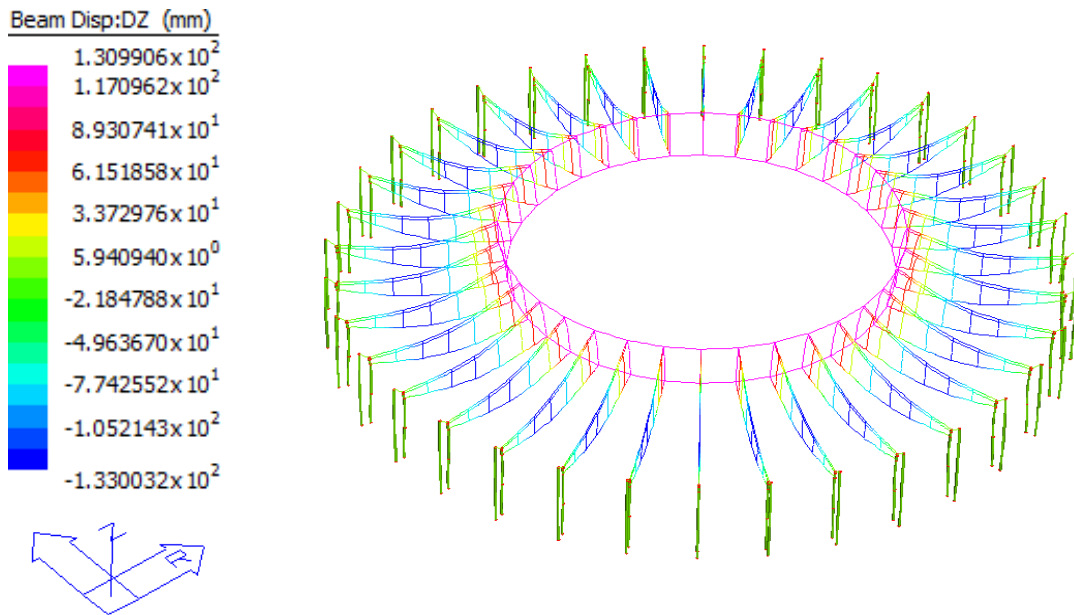


FIGURE 4. Vertical displacements for linear static

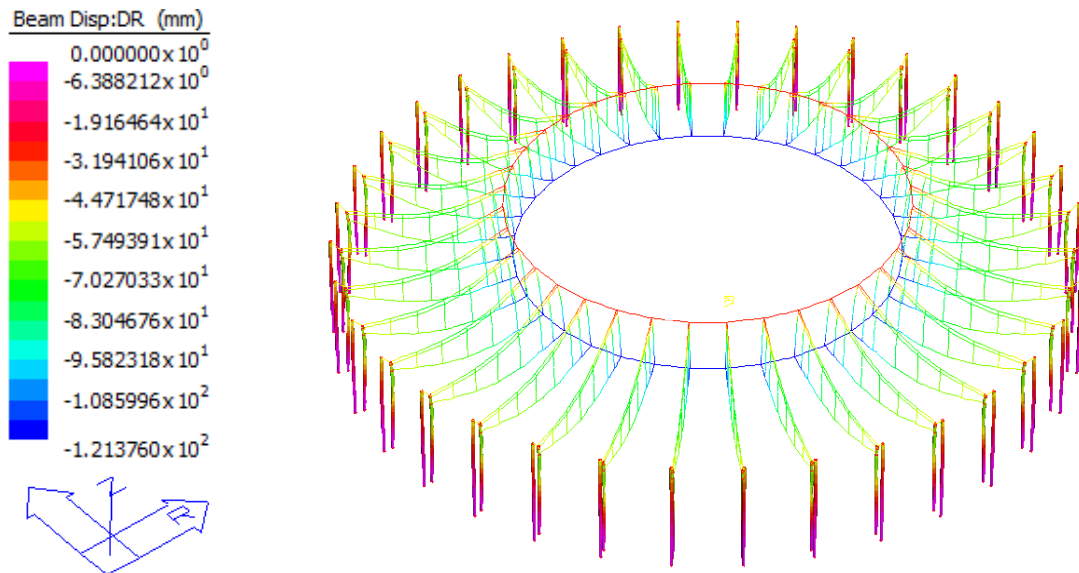


FIGURE 5. Radial displacements for linear static

FIGURE 4 shows a maximum deflection of 133 mm downward under self-weight and post-tension, well under the design limit of 450mm for serviceability. There is also an upward deflection of 131 mm induced by the tension in the bottom chord cable. FIGURE 5 shows the inner ring contracting inwards 121 mm in equilibrium. This contraction is due to the net resultant force of the inner ring in tension.

Linear Transient Dynamic Solver

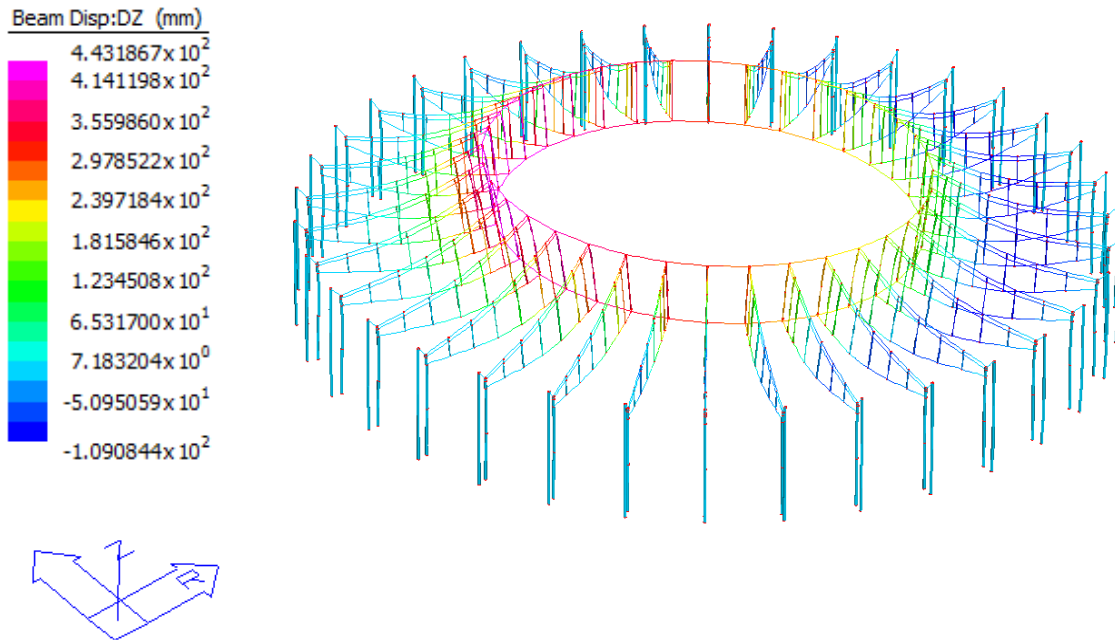


FIGURE 6. Vertical displacement for Linear Transient Dynamic Solver

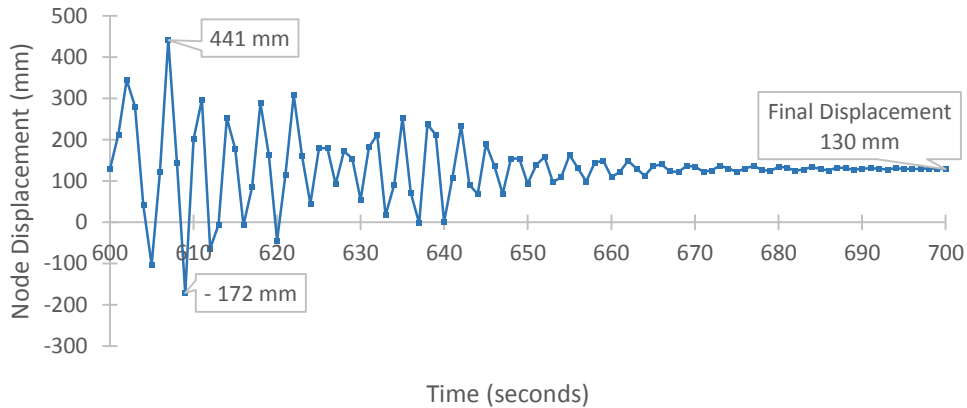


FIGURE 7. Vertical displacement El Centro

It was found no members reached yield capacity. The worst case base acceleration for El-Centro Earthquake occurred in the vertical direction, other directions were not critical. Due to symmetry, the maximum displacement is expected at the free end of the cantilever. FIGURE 6 shows this maximum beam displacement to be -109 mm in the Z direction. Note that this is different from the node displacement in FIGURE 7 of -172 mm. The final node displacements after the earthquake were equivalent to the linear static solver of 130 mm where the structure was in equilibrium as shown in FIGURE 7. These are below the AS1170.0 limit of 450 mm.

A Non-Linear Transient Dynamic Solver would account for deformed geometry. However following an initial simulation, this was found to be a time-consuming computation with non-convergence of time steps. A Linear Transient Dynamic Solver was chosen as it was time efficient.

STRUCTURAL DESIGN

TABLE 4 compares theoretical loadings using AS4100 with the Strand7 results. The calculations for AS4100 theoretical maximums are listed in APPENDIX 1.

TABLE 4. Strand7 results compared with AS4100 Serviceability requirements

Loading Type	Critical Member	Size	AS 4100 Maximum	Strand7 Results
Flexure	Top Chord	250x30 CHS	$M_i = 284 \text{ kNm}$	$M^* = 226 \text{ kNm}$
Axial	Column	800x50 CHS	$\phi N_c = 15624 \text{ kN}$	$N_c^* = 490 \text{ kN}$
Compression				
Axial Tension (Cables)	Inner Ring	10 mm Cable	$\phi N_t = 2142 \text{ kN}$	$N_t^* = 1551 \text{ kN}$
Axial Tension (Beams)	Top chord	250x30 CHS	$\phi N_t = 5971 \text{ kN}$	$N_t^* = 225 \text{ kN}$
Deflection	Top Chord	250x30 CHS	$\delta = 450 \text{ mm}$	$\delta^* = 133 \text{ mm}$
Critical Buckling Case	Column	800x50 CHS	$P_{crit} = 3894 \text{ kN}$	$P^* = 710 \text{ kN}$

CONCLUSIONS

The complex column structure was successfully simplified into a 2D model and rotated through 360° to create the 3D structure. The deflection of the cantilevers was the key criteria of design. Design aims for deflection, buckling and earthquake were satisfied. Axial loads and bending moments were checked after deflection was satisfied. Net upward deflections at the end of the cantilever were achieved with the use of tensioned cable elements and tapered out truss geometry which allowed flexibility of the bottom chord of the truss. The Teflon roof membrane was an efficient choice as a roof membrane as it fully restrained the top chord without contributing a large dead load. The combined action of buckling and axial load proved to be critical for the columns. There was sufficient capacity to handle self-weight and the El-Centro earthquake. The innovation of using tensioned cables in a bottom inner ring allowed for a long span cantilever roof.

REFERENCES

- CMC (2010). *Code for Seismic Design of Buildings (GB50011-2010)*. China Ministry of Construction, China Architecture and Building Press: Beijing, China. (in Chinese)
- Frearson, A., 2011. De Zeen Magazine. [Online]. Available at: <http://www.dezeen.com/2011/08/16/baoan-stadium-by-gmp-architekten>. [Accessed 12 May 2016].
- Guo, Y., Tian, G., Wang, K., Zhang, B., & Zhao, S. (2011). Tensioning experiment on spoke structural roof of Bao'An Stadium. *Journal of Building Structures*, 32(3), 1-10.
- Guo, Y., Wang, K., Sun, W., Tian, G., & Zhang, B. (2013). Research on key structural design problems of the Bao'An Stadium. *Journal of Building Structures*, 5 (1) 11-20.
- Ronstan (2011). *RPA112 Structural Cable Catalogue*. Adelaide, Australia.
- Standards Association of Australia (1998). *AS 4100 Steel Structures*, Sydney, Australia.
- Standards Association of Australia (2002). *AS1170.0 Structural Design Actions Part 0: General Principles*. Sydney, Australia.
- Strand 7 (2011). *ST7-1.40.35.3 Analysing Membrane Structures*. Sydney, Australia
- Strand 7 (2011). *ST7-1.40.35.8 Modelling Tension-Only or Compression-Only Structural Members*. Sydney, Australia
- Tian, G., Guo, Y., Zhang, B., Wang, K., & Zhao, S. (2011). Experiment on sensitivity to construction tolerance and research on tolerance control criteria in spoke structural roof of Bao'An Stadium. *Journal of Building Structures*, 32(3), 11-18.

APPENDIX 1

External Column

Axial Compression

Member subjected to axial compression design as per AS 4100

$A_g = 117810 \text{ mm}^2$, $I = 8.32 \times 10^9 \text{ mm}^4$, $k_f = 1$, $f_{yf} = 320 \text{ MPa}$, $f_u = 440 \text{ MPa}$

For compression $\phi = 0.9$ (Table 3.4)

Nominal Section Capacity (Clause 6.2.1)

$$\phi N_s = \phi k_f A_g f_y = 0.9 \times 1 \times 117810 \times 320 = 32,929.3 \text{ kN}$$

Nominal Member Capacity (Clause 6.3.3)

$$\lambda_n = \frac{l_e}{r} \sqrt{k_f} \sqrt{\frac{f_y}{250}} = \frac{30000}{\sqrt{\left(\frac{8.32 \times 10^9}{117810}\right)}} \sqrt{1} \left(\sqrt{\frac{320}{250}} \right) = 127.38$$

$\alpha_b = -1.0$ $\alpha_c = 0.4605$ (Table 6.3.3.3)

$$\therefore \phi N_{cx} = 0.4605 \times 32,929.3 = 15624.4 \text{ kN}$$

$$\therefore \phi N_s = 32,929.3 \text{ kN and } \phi N_c = 15624.4 \text{ kN}$$

Axial Tension

Yield capacity (Clause 7.2)

$$\phi N_y = \phi A_g f_y = 0.9 \times 117810 \times 320 = 32,929.3 \text{ kN}$$

Combined Actions

$$Z_e = \frac{I}{y_{max}} = \frac{8.32 \times 10^9}{400} = 20.8 \times 10^6 \text{ mm}^3 \quad S = \frac{\pi(d_{out}^4 - d_{in}^4)}{32 d_{out}} = \frac{\pi(800^4 - 700^4)}{32 \times 800} = 20.8 \times 10^9 \text{ mm}^3$$

$Z_c = \min[S, 1.5Z_e] = 20.8 \times 10^9$, $k_f = 1$, $f_{yf} = 320 \text{ MPa}$, $f_u = 440 \text{ MPa}$, $N^* = 710 \text{ kN}$, $M^* = 1298 \text{ kNm}$

$$M_s = f_y Z_e = 320 \times 20.8 \times 10^6 = 6656 \text{ kNm}$$

Section capacity (Clause 8.3.2) and in-plane capacity (Clause 8.4.2.2)

$$\phi M_r = \phi M_s \left(1 - \frac{N^*}{\phi N_s} \right) = 0.9 \times 6656 \left(1 - \frac{710}{32,929.3} \right) = 5865 \text{ kNm}$$

$$\phi M_i = \phi M_s \left(1 - \frac{N^*}{\phi N_c} \right) = 0.9 \times 6656 \left(1 - \frac{710}{15624.4} \right) = 5718.2 \text{ kNm}$$

SATSIFACTORY

Top Chord

Axial Compression

Member subjected to axial compression design as per AS 4100

$A_g = 20734.5 \text{ mm}^2$, $I = 1.2778 \times 10^8 \text{ mm}^4$, $k_f = 1$, $f_{yf} = 320 \text{ MPa}$, $f_u = 440 \text{ MPa}$

For compression $\phi = 0.9$ (Table 3.4)

Nominal Section Capacity (Clause 6.2.1)

$$\phi N_s = \phi k_f A_g f_y = 0.9 \times 1 \times 20734.5 \times 320 = 5971 \text{ kN}$$

Nominal Member Capacity (Clause 6.3.3)

$$\lambda_n = \frac{l_e}{r} \sqrt{k_f} \sqrt{\frac{f_y}{250}} = \frac{8630}{\sqrt{\left(\frac{1.2778 \times 10^8}{20734.5}\right)}} \sqrt{1} \left(\sqrt{\frac{320}{250}} \right) = 124$$

$\alpha_b = -1.0$ $\alpha_c = 0.476$ (Table 6.3.3.3)

$$\therefore \phi N_{cx} = 0.476 \times 5971 = 2842.2 \text{ kN}$$

$$\therefore \phi N_s = 5971 \text{ kN and } \phi N_c = 2842.2 \text{ kN}$$

Axial Tension

Yield capacity (Clause 7.2)

$$\phi N_y = \phi A_g f_y = 0.9 \times 20734.5 \times 320 = 5971 \text{ kN}$$

Combined Actions

$$Z_e = \frac{I}{y_{max}} = \frac{1.2778 \times 10^8}{125} = 1022 \times 10^3 \text{ mm}^3 \quad S = \frac{\pi(d_{out}^4 - d_{in}^4)}{32 d_{out}} = \frac{\pi(250^4 - 190^4)}{32 \times 250} = 1022 \times 10^3 \text{ mm}^3$$

$Z_c = \min[S, 1.5Z_e] = 1022 \times 10^3$, $k_f = 1$, $f_{yf} = 320 \text{ MPa}$, $f_u = 440 \text{ MPa}$, $N^* = 225 \text{ kN}$, $M^* = 226 \text{ kNm}$

$$M_s = f_y Z_e = 320 \times 1022 \times 10^3 = 327 \text{ kNm}$$

Section capacity (Clause 8.3.2) and in – plane capacity (Clause 8.4.2.2)

$$\phi M_r = \phi M_s \left(1 - \frac{N^*}{\phi N_s}\right) = 0.9 \times 327 \left(1 - \frac{225}{5971}\right) = 290 \text{ kNm}$$

$$\phi M_i = \phi M_s \left(1 - \frac{N^*}{\phi N_c}\right) = 0.9 \times 327 \left(1 - \frac{225}{2842.2}\right) = 284 \text{ kNm}$$

SATISFACTORY

Box Girder

Axial Compression

Member subjected to axial compression design as per AS 4100

$A_g = 20000 \text{ mm}^2$, $I_x = 1.667 \times 10^7 \text{ mm}^4$, $I_y = 6.667 \times 10^7 \text{ mm}^4$, $k_f = 1$, $f_{yf} = 320 \text{ MPa}$, $f_u = 440 \text{ MPa}$

For compression $\phi = 0.9$ (Table 3.4)

Nominal Section Capacity (Clause 6.2.1) X AXIS

$$\phi N_s = \phi k_f A_g f_y = 0.9 \times 1 \times 20000 \times 320 = 5760 \text{ kN}$$

Nominal Member Capacity (Clause 6.3.3)

$$\lambda_{nx} = \frac{l_e}{r} \sqrt{k_f} \sqrt{\frac{f_y}{250}} = \frac{4243}{\sqrt{\left(\frac{1.667 \times 10^7}{20000}\right)}} \sqrt{1} \left(\sqrt{\frac{320}{250}}\right) = 5.76$$

$$\alpha_b = -1.0 \quad \alpha_c = 1 \text{ (Table 6.3.3.3)}$$

$$\therefore \phi N_{cx} = \phi N_{sx} = 5760 \text{ kN}$$

Y AXIS

$$\lambda_{ny} = \frac{l_e}{r} \sqrt{k_f} \sqrt{\frac{f_y}{250}} = \frac{4243}{\sqrt{\left(\frac{6.667 \times 10^7}{20000}\right)}} \sqrt{1} \left(\sqrt{\frac{320}{250}}\right) = 83.14$$

$$\alpha_b = -1.0$$

$$\alpha_c = 0.7885 \text{ (Table 6.3.3.3)}$$

$$\therefore \phi N_{cy} = 0.7885 \times 5760 = 4541.76 \text{ kN}$$

$$\therefore \phi N_s = 5760 \text{ kN}, \phi N_{cx} = 5760 \text{ kN} \text{ and } \phi N_{cy} = 4541.76 \text{ kN}$$

Axial Tension

Yield capacity (Clause 7.2)

$$\phi N_y = \phi A_g f_y = 0.9 \times 20000 \times 320 = 5760 \text{ kN}$$

Combined Actions

$$Z_{ex} = \frac{I}{y_{max}} = \frac{1.667 \times 10^7}{50} = 333 \times 10^3 \text{ mm}^3 \quad Z_{ey} = \frac{I}{y_{max}} = \frac{6.667 \times 10^7}{100} = 667 \times 10^3 \text{ mm}^3$$

$$S_x = \frac{bh^2}{6} = \frac{200 \times 100^2}{6} = 333.3 \times 10^3 \text{ mm}^3 \quad S_y = \frac{b^2 h}{6} = \frac{200^2 \times 100}{6} = 666.7 \times 10^3 \text{ mm}^3$$

$Z_{ex} = \min[S, 1.5Z_e] = 333 \times 10^3$, $Z_{ey} = \min[S, 1.5Z_e] = 666.7 \times 10^3$ $k_f = 1$, $f_{yf} = 320 \text{ MPa}$, $f_u = 440 \text{ MPa}$, $N^* = 12.8 \text{ kN}$, $M^* = 5.22 \text{ kNm}$

$$M_{sx} = f_y Z_e = 320 \times 333 \times 10^3 = 107 \text{ kNm}$$

Section capacity (Clause 8.3.2) and in – plane capacity (Clause 8.4.2.2)

$$\phi M_r = \phi M_s \left(1 - \frac{N^*}{\phi N_s}\right) = 0.9 \times 107 \left(1 - \frac{12.8}{5760}\right) = 96 \text{ kNm}$$

$$\phi M_i = \phi M_s \left(1 - \frac{N^*}{\phi N_c}\right) = 0.9 \times 107 \left(1 - \frac{12.8}{5760}\right) = 96 \text{ kNm}$$

SATISFACTORY

Vertical Truss Member

Axial Compression

Member subjected to axial compression design as per AS 4100

$A_g = 12252.2 \text{ mm}^2$, $I = 2.33 \times 10^8 \text{ mm}^4$, $k_f = 1$, $f_{yf} = 320 \text{ MPa}$, $f_u = 440 \text{ MPa}$

For compression $\phi = 0.9$ (Table 3.4)

Nominal Section Capacity (Clause 6.2.1)

$$\phi N_s = \phi k_f A_g f_y = 0.9 \times 1 \times 12252.2 \times 320 = 3528.6 \text{ kN}$$

Nominal Member Capacity (Clause 6.3.3) assume largest length **16245mm**

$$\lambda_{nx} = \frac{l_e}{r} \sqrt{k_f} \sqrt{\frac{f_y}{250}} = \frac{16245}{\sqrt{\left(\frac{2.33 \times 10^8}{12252.2}\right)}} \sqrt{1} \left(\sqrt{\frac{320}{250}}\right) = 1$$

$$\alpha_b = -1.0 \quad \alpha_c = 1 \quad (\text{Table 6.3.3.3})$$

$$\therefore \phi N_{cx} = \phi N_{sx} = 3528.6 \text{ kN}$$

Axial Tension

Yield capacity (Clause 7.2)

$$\phi N_y = \phi A_g f_y = 0.9 \times 12252.2 \times 320 = 3528.6 \text{ kN}$$

Combined Actions

$$Z_e = \frac{I}{y_{max}} = \frac{2.33 \times 10^8}{200} = 1165 \times 10^3 \text{ mm}^3 \quad S = \frac{\pi(d_{out}^4 - d_{in}^4)}{32d_{out}} = \frac{\pi(400^4 - 380^4)}{32 \times 400} = 1165 \times 10^3 \text{ mm}^3$$

$$Z_{ex} = \min[S, 1.5Z_e] = 1165 \times 10^3, \quad k_f = 1, \quad f_{yf} = 320 \text{ MPa}, \quad f_u = 440 \text{ MPa}, \quad N^* = 14 \text{ kN}, \quad M^* = 100 \text{ kNm}$$

$$M_{Sx} = f_y Z_e = 320 \times 1165 \times 10^3 = 373 \text{ kNm}$$

Section capacity (Clause 8.3.2) and in-plane capacity (Clause 8.4.2.2)

$$\phi M_r = \phi M_s \left(1 - \frac{N^*}{\phi N_s}\right) = 0.9 \times 373 \left(1 - \frac{14}{3528.6}\right) = 334 \text{ kNm}$$

$$\phi M_i = \phi M_s \left(1 - \frac{N^*}{\phi N_c}\right) = 0.9 \times 373 \left(1 - \frac{14}{3528.6}\right) = 334 \text{ kNm}$$

SATISFACTORY

Inner Ring Cable

Axial Tension

For a 50mm diameter ACS4 structural cable $f_{yf} = 1212 \text{ MPa}$ (Ronstan, 2011)

Yield capacity (Clause 7.2)

$$\phi N_y = \phi A_g f_y = 0.9 \times 1964 \times 1212 = 2142 \text{ kN}$$

Bottom Chord

Axial Compression

Member subjected to axial compression design as per AS 4100

$$A_g = 3063.05 \text{ mm}^2, \quad I = 1.457 \times 10^7 \text{ mm}^4, \quad k_f = 1, \quad f_{yf} = 320 \text{ MPa}, \quad f_u = 440 \text{ MPa}$$

For compression $\phi = 0.9$ (Table 3.4)

Nominal Section Capacity (Clause 6.2.1)

$$\phi N_s = \phi k_f A_g f_y = 0.9 \times 1 \times 3063.05 \times 320 = 882 \text{ kN}$$

Nominal Member Capacity (Clause 6.3.3)

$$\lambda_n = \frac{l_e}{r} \sqrt{k_f} \sqrt{\frac{f_y}{250}} = \frac{8550}{\sqrt{\frac{1.457 \times 10^7}{3063.05}}} \sqrt{1} \left(\sqrt{\frac{320}{250}} \right) = 140$$

$$\alpha_b = -1.0 \quad \alpha_c = 0.389 \quad (\text{Table 6.3.3.3})$$

$$\therefore \phi N_{cx} = 0.389 \times 882 = 343 \text{ kN}$$

$$\therefore \phi N_s = 882 \text{ kN and } \phi N_c = 343 \text{ kN}$$

Axial Tension

Yield capacity (Clause 7.2)

$$\phi N_y = \phi A_g f_y = 0.9 \times 3063.05 \times 320 = 882 \text{ kN}$$

Combined Actions

$$Z_e = \frac{I}{y_{max}} = \frac{1.457 \times 10^7}{100} = 146 \times 10^3 \text{ mm}^3 \quad S = \frac{\pi(d_{out}^4 - d_{in}^4)}{32d_{out}} = \frac{\pi(200^4 - 190^4)}{32 \times 200} = 146 \times 10^3 \text{ mm}^3$$

$$Z_e = \min[S, 1.5Z_e] = 146 \times 10^3, \quad k_f = 1, \quad f_{yf} = 320 \text{ MPa}, \quad f_u = 440 \text{ MPa}, \quad N^* = 53.33 \text{ kN}, \quad M^* = 30 \text{ kNm}$$

$$M_s = f_y Z_e = 320 \times 146 \times 10^3 = 47 \text{ kNm}$$

Section capacity (Clause 8.3.2) and in-plane capacity (Clause 8.4.2.2)

$$M_r = \phi M_s \left(1 - \frac{N^*}{\phi N_s}\right) = 0.9 \times 47 \left(1 - \frac{53.33}{882}\right) = 40 \text{ kNm}$$

$$M_i = \phi M_s \left(1 - \frac{N^*}{\phi N_c}\right) = 0.9 \times 47 \left(1 - \frac{53.33}{343}\right) = 35 \text{ kNm}$$

SATISFACTORY